ACS central science

http://pubs.acs.org/journal/acscii

Research Article

Assessing Antigen Structural Integrity through Glycosylation Analysis of the SARS-CoV-2 Viral Spike

Juliane Brun,[§] Snežana Vasiljevic,[§] Bevin Gangadharan,[§] Mario Hensen,[§] Anu V. Chandran, Michelle L. Hill, J.L. Kiappes, Raymond A. Dwek, Dominic S. Alonzi, Weston B. Struwe,* and Nicole Zitzmann*

Cite This: *ACS Cent. Sci.* 2021, 7, 586−593

Read Online

ACCESS | Metrics & More | Article Recommendations | Supporting Information

ABSTRACT: Severe acute respiratory syndrome coronavirus 2 is the causative pathogen of the COVID-19 pandemic which as of March 29, 2021, has claimed 2 776 175 lives worldwide. Vaccine development efforts focus on the viral trimeric spike glycoprotein as the main target of the humoral immune response. Viral spikes carry glycans that facilitate immune evasion by shielding specific protein epitopes from antibody neutralization, and antigen efficacy is influenced by spike glycoprotein production in vivo. Therefore, immunogen integrity is important for glycoprotein-based vaccine candidates. Here, we show how site-specific glycosylation differs between virus-derived spikes, wild-type, non-stabilized spikes expressed from a plasmid with a CMV promoter and tPA signal sequence, and commonly used recombinant, engineered spike glycoproteins. Furthermore, we show that their distinctive cellular secretion pathways result in different protein glycosylation and secretion patterns, including shedding of spike monomeric subunits for the non-stabilized wild-type spike tested, which may have implications for the resulting immune response and vaccine design.

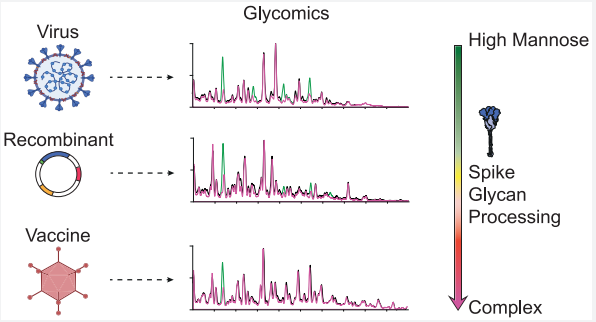

Severe acute respiratory syndrome coronavirus 2 (SARS-CoV-2), the causative agent of coronavirus disease 2019 (COVID-19), can induce fever, severe respiratory illness, and various multiorgan disease manifestations. The virus enters host cells by binding to angiotensin-converting enzyme 2 (ACE-2) using its extensively glycosylated spike (S) protein.[1,2] The S glycoprotein is a class I fusion protein, comprising two functional subunits; the S1 subunit is responsible for ACE-2 receptor binding, and the S2 subunit initiates membrane fusion between the virus particle and host cell. The surface of each trimeric spike displays up to 66 N-linked glycans and an undefined number of O-linked glycans.[3] Protruding trimeric spikes on viruses are key targets for the natural immune response.[4] Neutralizing antibodies that target these spikes, especially the S1 domain, prevent cellular uptake of viruses by the host, and consequently, most vaccine design efforts focus on the S protein.

Host-derived glycosylation plays many important roles in viral pathobiology, including mediating viral protein folding and stability, as well as influencing viral tropism and immune evasion.[5] Understanding how SARS-CoV-2 exploits glycosylation on native S proteins will help guide rational vaccine design, as glycans enable immune evasion by shielding underlying immunogenic protein epitopes from antibody neutralization,[6] as also observed for other coronaviruses.[7,8] In other instances, glycans constitute functional epitopes in immune recognition,[9] further highlighting the need for molecular mimicry between the virus and vaccines that are designed to prime the immune system by eliciting neutralizing antibodies. Importantly, several COVID-19 vaccine candidates are based on viral vectors encoding SARS-CoV-2 S protein, including ChAdOx1 nCoV-19 (AZD1222).[10,11]

We observed profound differences in the glycosylation of the recombinant non-stabilized wild-type spike compared to the wild-type virus. To fully appreciate the basis for these alterations, it is important to examine the biosynthesis, assembly, and secretion of SARS-CoV-2 S glycoprotein trimers in the context of a viral infection. S protein synthesis in the endoplasmic reticulum (ER) of an infected cell is accompanied by cotranslational addition of preassembled N-glycans to its 22 N-glycosylation sites.[12] After trimerization and initial N-glycan processing in the ER by resident sugar modifying enzymes, membrane anchored S trimers travel to the ER−Golgi intermediate compartment (ERGIC) where they are incorporated into viruses budding into the ERGIC lumen.[13,14] S

Received: January 14, 2021
Published: March 31, 2021

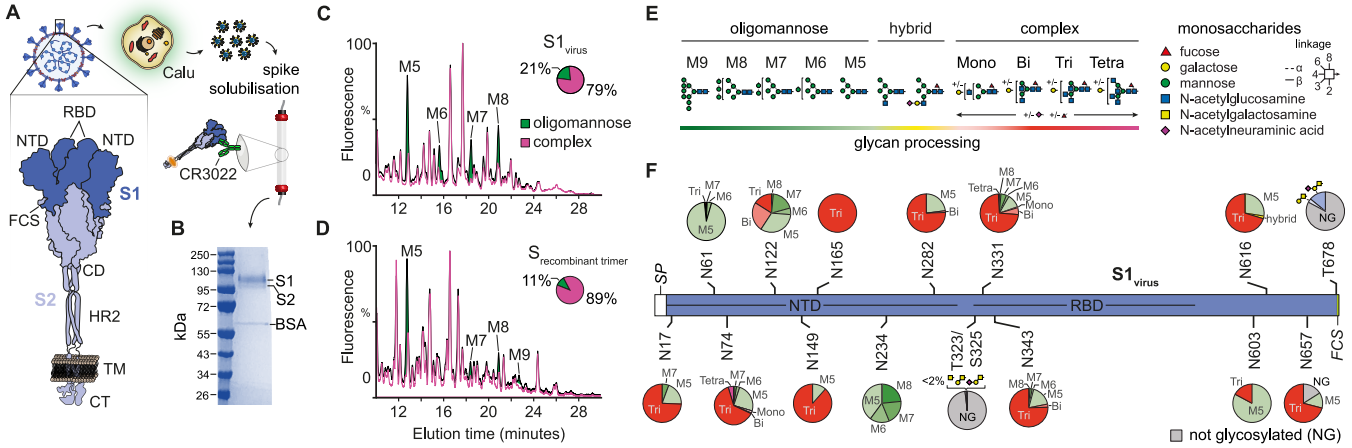

Figure 1. Purification and glycan analysis of the SARS-CoV-2 spike glycoprotein. (A) Schematic representation of spike purification from SARS-CoV-2 infected Calu-3 cells by immunoaffinity purification using the S1 targeting CR3022 antibody. Spike S1 and S2 subunits are colored dark and light blue, respectively, with receptor binding domain (RBD), N-terminal domain (NTD), furin cleavage site (FCS), connecting domain (CD), heptad repeat 2 (HR2), transmembrane domain (TM), and cytoplasmic tail (CT) labeled. (B) SDS-PAGE showing the presence of S1 and S2 subunits of virus-derived spike. Quantitative UHPLC N-glycan analysis showing the distribution of oligomannose and complex-type glycans on $S1_{virus}$ (C) and $S_{recombinant\text{-}trimer}$ (D). (E) N-glycan maturation showing color coding for degree of glycan processing from oligomannose (green) to hybrid (yellow) to complex (purple). (F) Quantitative site-specific N- and O-glycosylation by bottom-up glycoproteomics of $S1_{virus}$. Pie charts depict the degree of N-glycan processing depicted in part E.

trimers protrude from the viral surface while individual viruses move along inside the lumina of cis-, medial- and trans-Golgi, where their N-glycans are extensively processed by Golgi resident glycosylation enzymes. O-glycans are also added in the Golgi, starting with the addition of GalNAc residues via GalNAc-transferase that can be further modified, similarly to N-glycans, across the Golgi stack. In the trans-Golgi, S trimers encounter the host protease furin that cleaves between S1 and S2,[15,16] leaving the subunits on S trimers noncovalently associated before the virus is secreted via lysosomes into the extracellular surrounding, completing the replication cycle.[17] Any alterations in the glycosylation pattern of secreted spike protein reflect changes in protein accessibility to the various enzymes of the cellular glycosylation machinery.[18,19] Such glycan signatures carry important information, for example, about the conformational and oligomerization state of the secreted protein.

Here, we correlate these principles, together with both quantitative and site-specific glycan analysis, to uncover unique signatures, and the mechanisms by which they originate, of S glycoproteins produced from (1) the SARS-CoV-2 virus, (2) a stabilized recombinant trimer, and (3) a recombinant non-stabilized wild-type spike construct with a tissue plasminogen activator (tPA) leader in a plasmid with a CMV promoter. We uncover not only that glycosylation differs among these systems but also critically that the majority of the S1 subunit is shed in a monomeric soluble form during cellular expression using a plasmid encoding the non-stabilized trimer. We believe that these differences could influence the efficacy of a vaccine that does not use a trimer stabilization strategy.

RESULTS AND DISCUSSION

Glycosylation of Spike S1 Isolated from Infectious Virions. To establish the authentic glycosylation of SARS-CoV-2 S, we grew virus (England/02/2020 strain) in Calu-3 lung epithelial cells, harvested the virus containing supernatant, and immunopurified detergent-solubilized spike using the cross-reactive CR3022 antibody that targets the receptor binding domain (RBD) on S (Figure 1A). Immunopurified material was analyzed by SDS-PAGE (Figure 1B). The protein bands corresponding to S1 (herein referred to as $S1_{virus}$) and S2 were excised and confirmed by mass spectrometry (Figure S1A). S2 protein levels were insufficient for additional glycan/glycoproteomics analysis. Quantitative N-glycan analysis via ultra-high-performance liquid chromatography (UHPLC)[39] of the $S1_{virus}$ showed a predominant population of complex-type N-glycans (79%) with 21% oligomannose and/or hybrid structures (Figure 1C). Comparing these values to a soluble recombinant trimeric form of S ($S_{recombinant\text{-}trimer}$), which has been engineered to both maintain a prefusion state and abolish the furin cleavage site (Figure S2)[20] and therefore also contains S2 N-glycans,[21] revealed $S_{recombinant\text{-}trimer}$ to carry only 11% oligomannose/hybrid and 89% complex N-glycans (Figure 1D).

This observation is significant as it indicates marked differences in glycan processing, a complex pathway that is influenced by glycan density and local protein architecture, both of which can sterically impair glycan maturation (Figure 1E). Changes in glycan maturation, resulting in the presence of oligomannose-type glycans, can be a sensitive reporter of nativelike protein architecture[22,23] and is also an important indicator for quality control and efficacy of different immunogens.[24]

To pinpoint where, and the extent to which, differences in glycan processing occur, we performed a quantitative site-specific glycosylation analysis of $S1_{virus}$ (Figure 1F) and $S_{recombinant\text{-}trimer}$ (Figure S3) by mass spectrometry. We detected glycopeptides for all 13 potential N-glycosylation sites in S1, and importantly, we found that S1 N-glycan processing is comparable between virus and recombinant material, excluding the possibility that differences in glycan processing observed by UHPLC are outweighed by the presence of the S2 subunit on $S_{recombinant\text{-}trimer}$. Looking closer at $S1_{virus}$, we observed three N-glycan sites, N61, N234, and N603, that are predominantly occupied by underprocessed oligomannose structures and are likely shielded by the quaternary spike structure. This is in

https://doi.org/10.1021/acscentsci.1c00058
ACS Cent. Sci. 2021, 7, 586−593

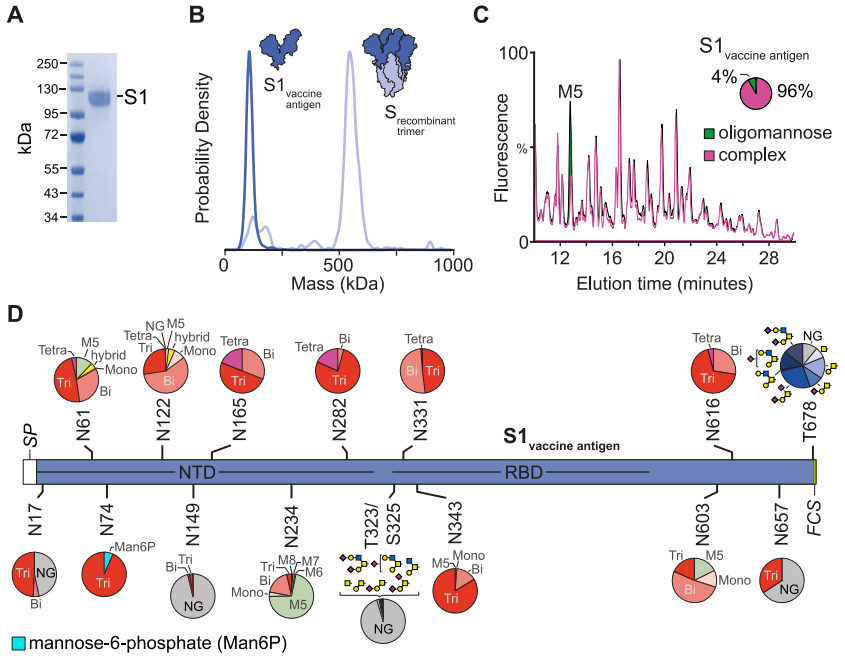

Figure 2. Glycosylation and assembly of a non-stabilized spike with a tPA leader sequence.. (A) SDS-PAGE of CR3022 purified $S1_{vaccine\text{-}antigen}$. (B) Mass photometry of monomeric $S1_{vaccine\text{-}antigen}$ (~120 kDa) and $S_{recombinant\text{-}trimer}$ (~550 kDa). (C) Quantitative UHPLC N-glycan analysis of $S1_{vaccine\text{-}antigen}$ showing the degree of glycan processing. (D) Site-specific N- and O-glycosylation of $S1_{vaccine\text{-}antigen}$ (see Figure 1E for the pie chart legend).

contrast to a preliminary previously reported N-glycan analysis on virus-derived S, where N61 carried mostly complex-type (with some oligomannose) glycans; N234 was a mixture of oligomannose, hybrid, and complex structures, and N603 was mostly complex.[25] We found that the remaining sites on $S1_{virus}$ were occupied either almost entirely by triantennary N-glycans (N149 and N165) or by a mixture of triantennary complex plus oligomannose (namely, $Man_5GlcNAc_2$, i.e., M5) structures. We did not detect any O-linked glycosylation at T232/S325 on $S_{recombinant\text{-}trimer}$, a feature that is variably reported among recombinant S or S1 material.[25−28] However, we identified O-glycosylation at T678 on $S1_{virus}$, which was absent on $S_{recombinant\text{-}trimer}$. This is particularly informative, indicating that this domain on $S1_{virus}$ is more accessible to GalNAc-transferases in the Golgi and that the viral spike is configured in a more open or flexible trimeric state than the recombinant, stabilized spike. We also observed the presence of SARS-CoV-2 nucleoprotein and SARS-CoV-2 membrane protein at lower levels in the immunopurified material (Table S1).

Comparative Analysis of Site-Specific Glycosylation on Non-Stabilized Spike. With the aim of comparing site-specific S glycosylation in the context of vaccine design and antigen structure to the viral spike glycoprotein above, we produced S in mammalian cells using an expression construct modeled on the one used in creating ChAdOx1 nCoV-19.[11] The construct contains SARS-CoV-2 amino acids 2−1273 preceded by an N-terminal leader peptide consisting of tPA and a modified human cytomegalovirus major (CMV) immediate early promoter.

Using the same purification strategy as above, we observed that the majority of overexpressed protein was secreted into the supernatant as soluble S1 (herein referred to as $S1_{vaccine\text{-}antigen}$), as detected by SDS-PAGE (Figure 2A) and confirmed by mass spectrometry (Figure S1B). S2 remained cell associated, embedded in the lipid bilayer, as shown by Western blot probed with an anti-S2 antibody (Figure S4). We analyzed the secreted $S1_{vaccine\text{-}antigen}$ by mass photometry and compared it to the stabilized $S_{recombinant\text{-}trimer}$, which revealed the shed S1 from non-stabilized trimers to be solely monomeric (Figure 2B, Movies S1 and S2).[38]

Glycan content analysis of $S1_{vaccine\text{-}antigen}$ demonstrated an extraordinary 96% of complex N-glycans and only 4% of oligomannose-type N-glycans (Figure 2C), indicating an increase in accessibility of glycan processing enzymes in the Golgi to $S1_{vaccine\text{-}antigen}$ glycan sites compared to $S1_{virus}$. Site-specific glycosylation analysis of $S1_{vaccine\text{-}antigen}$ confirmed that although overall N-glycan site occupancy was comparable to $S1_{virus}$, except for N17, which was 47% nonglycosylated, the large majority of N-glycans attached to $S1_{vaccine\text{-}antigen}$ underwent considerably more processing, likely after furin cleavage in the Golgi, as evidenced by the presence of increased complex glycosylation. The N61 and N603 sites, which were 98% and 83% oligomannose on $S1_{virus}$, became 12% and 18% on $S1_{vaccine\text{-}antigen}$, respectively. We also detected an increase in T323/S325 and T678 O-glycan extensions (i.e., presence of core-2 structures) as well as a 50% increase in sialylation at T678. Finally, N-glycan sites that had mixed oligomannose and complex glycan populations on $S1_{virus}$ (N74, N122, N343, and N616) become heavily processed on $S1_{vaccine\text{-}antigen}$ (Figures 1F and 2D for $S1_{virus}$ and $S1_{vaccine\text{-}antigen}$, respectively).

However, a single N-glycan site maintained an underprocessed structure. For $S1_{virus}$, 60% of N234 N-glycans were $Man_{6-8}GlcNAc_2$ (M6, M7, and M8). In contrast, although $S1_{vaccine\text{-}antigen}$ N234 carried the slightly more processed M5 N-glycan, the remaining structures at this site did not progress to more complex type glycosylation like the rest of S1 N-glycans. The prevention of glycan processing at N234 is due to the spatial and temporal assembly of S proteins in the ER and Golgi. On a fully assembled S trimer, N234 glycans are located in a pocket formed partly by the RBD and the N-terminal

https://doi.org/10.1021/acscentsci.1c00058
ACS Cent. Sci. 2021, 7, 586−593

domain (NTD) on the same protomer, and partly by a neighboring RBD, which prevents N-glycan trimming when S is present as a trimer in the ER (Figure 3A). In both

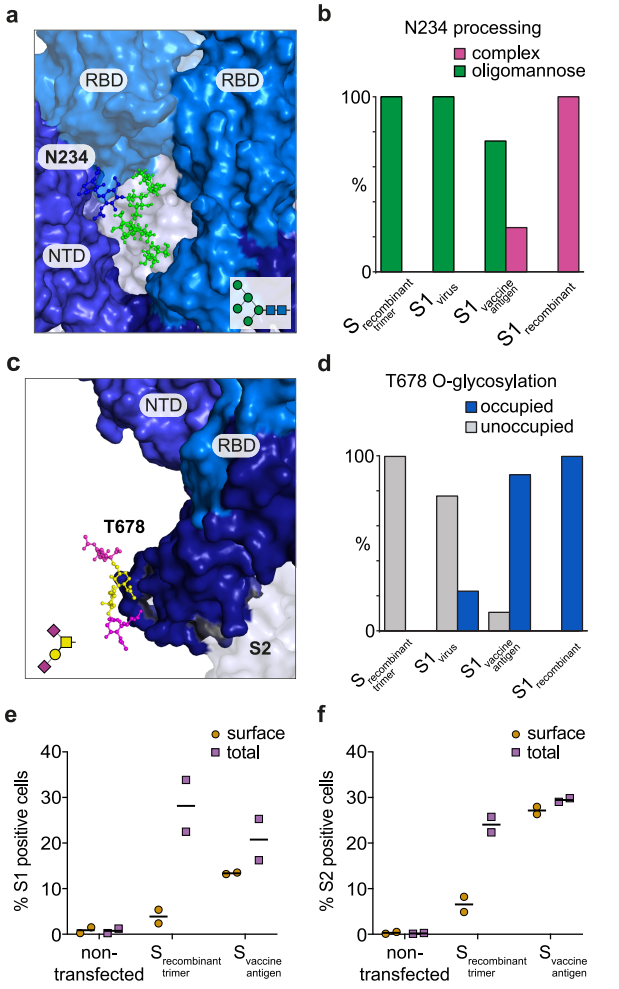

Figure 3. Correlation of spike cellular location and macromolecular assembly with N234 and T678 glycan processing. (A) Structural position and orientation of the S1 N-glycan N234 (shown as $Man_5GlcNAc_2$) in a pocket formed by the RBD (top-right corner) and NTD of the same protomer, and the neighboring RBD (top-left corner). The GLYCAM web server (http://glycam.org) was used to model the glycan onto the PDB 6VXX and rendered using PyMOL. (B) Percentage change in oligomannose content of the N234 N-glycan of $S_{recombinant\text{-}trimer}$, $S1_{virus}$, $S1_{vaccine\text{-}antigen}$, and $S1_{recombinant}$. (C) Location of the S1 O-glycan T678 (shown as disialylated core-1 structure) located in the subdomain (SD) near the furin cleavage site between S1 and S2 (modeled on PDB 6VXX using the GLYCAM web server) and rendered using PyMOL. (D) Changes in T678 O-glycan occupancy across samples tested. (E) Flow cytometry analysis of nontransfected and $S_{recombinant\text{-}trimer}$ and $S_{vaccine\text{-}antigen}$ transfected HEK293F cells stained positive for S1 or (F) S2 solely on the cell surface or in permeabilized cells. Data are shown as mean ± SEM (n = 2).

recombinant trimer-derived and viral S1, N234 was 100% oligomannose but dropped to 74.8% oligomannose on $S1_{vaccine\text{-}antigen}$ (Figure 3B). The fact that this site was also underprocessed on $S1_{vaccine\text{-}antigen}$ indicates that this subunit is derived from a spike that existed as a trimer in the ER, but a trimeric form that is seemingly less "closed" and more accessible to mannose-trimming ER enzymes as compared to its counterpart expressed by the SARS-CoV-2 virus.

This slightly less closed non-stabilized trimer travels from the ER to the ERGIC, but as there are no viruses present to incorporate these membrane-bound forms into their envelopes when budding into the ERGIC lumen, the overexpression system causes the $S_{vaccine\text{-}antigen}$ trimers to be pushed along the cis-, medial-, and trans-Golgi on their way to the cell surface. We detected mannose-6-phosphate (M-6-P) on $S1_{vaccine\text{-}antigen}$ (Figure 2D and Figure S5), evidenced from the same isotopic distribution and LC retention time for this modification that was also observed on $S1_{virus}$ (Figure S6). This sugar tag is initially added in the cis-Golgi in the form of GlcNAc-M-6-P; then, it is decapped in the trans-Golgi and recognized by the M-6-P receptor responsible for directing tagged proteins, and plausibly whole viruses, from the trans-Golgi to late endosomes/lysosomes; such lysosomal egress has recently been described for SARS-CoV-2.[17] With the furin cleavage site intact, $S_{vaccine\text{-}antigen}$ is cleaved by furin in the trans-Golgi; however, unlike endogenous viral spikes, where we postulate that additional stabilizing viral factors are present, $S1_{vaccine\text{-}antigen}$ dissociates from $S2_{vaccine\text{-}antigen}$ and becomes secreted. This shedding occurs in the trans-Golgi rather than at the plasma membrane of the cell, as evidenced by the increased N-glycan processing by late-stage Golgi glycosylation enzymes, resulting in the high complex-type N-glycan content of $S1_{vaccine\text{-}antigen}$, and also by the substantially increased O-glycosylation occupancy levels on T678 (Figure 3D and Figure S7). Plausibly, the modest amount of $S1_{virus}$ T678 O-glycosylation is related to furin cleavage, making $S1_{virus}$ more accessible to O-GalNAc-transferase; however, differences in virus assembly and the continuous association with, and shielding by, $S2_{virus}$ prevent this from reaching similar O-glycan occupancy levels as that of cleaved soluble $S1_{vaccine\text{-}antigen}$ (Figure 3D). Although $S_{recombinant\text{-}trimer}$ transits the trans-Golgi in a soluble form, it is not O-glycosylated at this position as it lacks the furin site (R682−R685, Figure 3C), cleavage of which appears to favor this processing step.

Glycan Processing of the Free Recombinant S1 Subunit. To test our hypothesis that $S1_{vaccine\text{-}antigen}$ comes from an assembled S trimer and is shed in the trans-Golgi following furin cleavage, we expressed the individual $S1_{recombinant}$ subunit (Figure S8), which cannot trimerize, and quantified the extent of N-glycan processing at N234 and O-glycosylation at T678. $S1_{recombinant}$ had 100% complex-type glycans at N234, shifting from 25% complex for $S1_{vaccine\text{-}antigen}$ and 0% for $S_{recombinant\text{-}trimer}$ and $S1_{virus}$ (Figure 3B). Similarly, T678 O-glycan occupancy was reversed from 0% ($S_{recombinant\text{-}trimer}$), 23% ($S1_{virus}$), and 90% ($S1_{vaccine\text{-}antigen}$) to 100% ($S1_{recombinant}$) (Figure 3D). The site-specific changes across all S1 samples are illustrated in Figure S9. However, cleavage of $S_{vaccine\text{-}antigen}$ by furin is not complete; around 10% was not O-glycosylated and appeared on the cell surface. Presence of S on the cell surface was shown by fluorescence activated cell sorting (FACS) analysis using staining with an S1- and S2-specific antibody of either unpermeabilized (i.e., surface localized S) or detergent-permeabilized cells (Figure 3E,F; Figure S10 and Table S2). It may be this likely trimerized and still S1-containing cell surface accessible spike is enough to give rise to an antibody response, as for example those reported in the ChAdOx1 nCoV-19 clinical trials.[10,11,29]

These results are encouraging, showing that it may be possible to improve on immunogen design. Shedding of

https://doi.org/10.1021/acscentsci.1c00058
ACS Cent. Sci. 2021, 7, 586−593

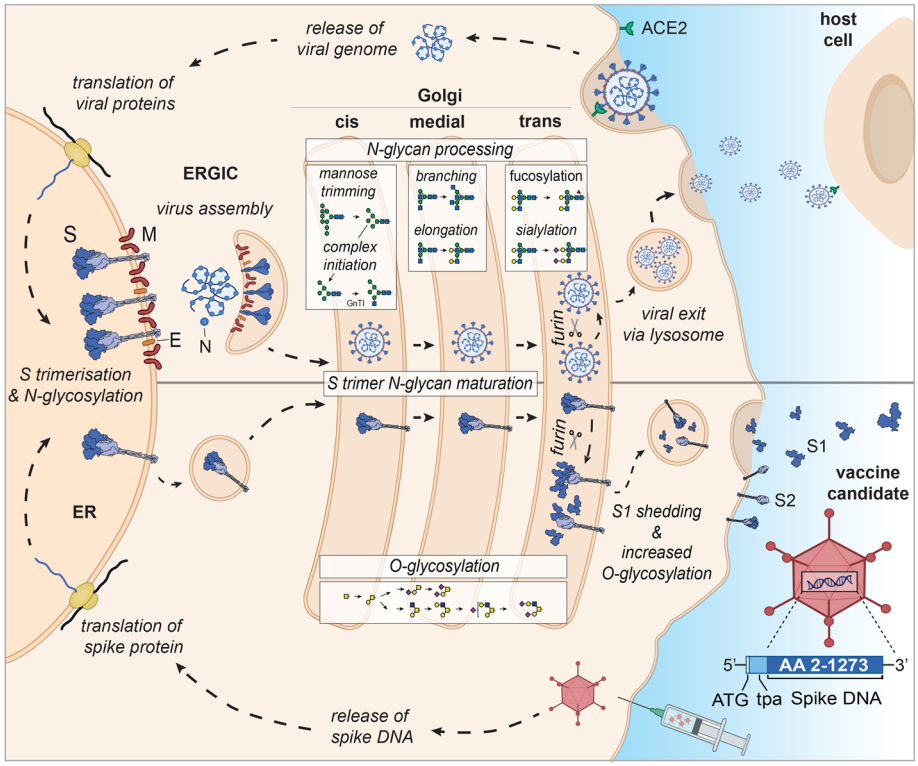

Figure 4. Differential expression and glycan processing of virions and non-stablized spike glycoproteins. SARS-CoV-2 binds to its receptor ACE-2 and infects cells, leading to the release of the viral genome and translation of viral proteins. Spike protein is cotranslationally N-glycosylated and forms trimers in the ER that traffic to the ERGIC where they are incorporated into budding virions. Individual virions continue through the secretory pathway to the trans-Golgi prior to following a lysosomal egress route. For any vaccine delivering DNA/RNA that results in a non-stabilized trimer, the spike is synthesized in the ER, where it is N-glycosylated and trimerizes as before, but as it is not incorporated into a budding virion in the ERGIC, it continues through the secretory pathway and, via lysosomes, to the plasma membrane. In both cases, the spike glycoproteins have access to both the N- and O-linked host glycosylation machinery. Upon furin cleavage in the trans-Golgi, S1 and S2 of the virus stay noncovalently associated, whereas furin cleavage of the non-stabilized spike results in shedding of monomeric $S1_{vaccine\text{-}antigen}$. Glycomic signature analysis of these two proteins shows that the N-linked glycosylation occupancy levels, which are determined in the ER, are comparable for $S1_{virus}$ and $S1_{vaccine\text{-}antigen}$ whereas the attached glycoforms vary reflecting their different accessibility to glycan processing enzymes. $S1_{vaccine\text{-}antigen}$ not only carries higher levels of complex N-glycans but is also extensively O-glycosylated after furin cleavage in the trans-Golgi, when most $S1_{vaccine\text{-}antigen}$ is shed and secreted in a soluble monomeric form. Some S1 and $S2_{vaccine\text{-}antigen}$ are displayed on the cell surface, presumably as trimers.

monomeric and nonphysiologically glycosylated $S1_{vaccine\text{-}antigen}$ from immunogen producing cells is reminiscent of HIV vaccine development, where early immunogens were hampered by the inability of monomeric gp120 to elicit a broadly neutralizing antibody response needed for virus neutralization.[30] Indeed, immunogens that do not mimic infectious virion trimeric spike glycoproteins may effectively act as a decoy, eliciting more of the unwanted suboptimal or non-neutralizing antibodies that are incapable of binding and neutralizing trimeric spikes on the virus.[9,30−32] Antibodies that neutralize by binding to the trimer apex will not be elicited by shed $S1_{vaccine\text{-}antigen}$ as it lacks the native protein architecture.

For example, S2M11[33] and C144[34] bind on a quaternary epitope formed by two neighboring RBDs at the trimer apex. Soluble monomeric S1 may also expose non-neutralizing epitopes, which are buried on assembled trimers. Furthermore, glycosylation at N234 affects the up/down orientation of the RBD domain and therefore ACE-2 binding.[3] Plausibly, enhanced glycan processing on shed $S1_{vaccine\text{-}antigen}$ could negatively affect antibody recognition due to a change in glycan charge and size (i.e., increase in sialic acid content and heightened branching) which may block peptide epitope.

CONCLUSIONS

A strong B-cell response is based on immunogen mimicry of an invading pathogen. Therefore, for the most effective SARS-CoV-2 vaccine, we suggest that a stabilized trimeric prefusion spike protein, with the furin cleavage site abolished, may be able to elicit neutralizing antibodies with the desirable significant breadth and potency. Viral vector-based vaccines, such as ChAdOx1 nCoV-19, as well as nucleic acid-based strategies, such as the Pfizer BNT162b2 and Moderna mRNA-1273 vaccines, rely on the antigen-encoding DNA or RNA sequence, once inside a cell, to produce spike proteins that faithfully resemble viral S, in both glycosylation and assembly, to elicit a robust innate immune response, as well as provoking T- and B-cells. However, the cellular secretion pathway followed by DNA/RNA-derived vaccine antigens may differ in fundamental ways from antigens present during viral infection, where factors other than a single protein coding sequence may play decisive roles in immunogen presentation (Figure 4). These include the (intra)cellular location of viral morphogenesis (i.e., from which organelle a virus buds), as well as the overall macromolecular assembly of an immunogen as it encounters the host glycosylation machinery during a natural infection. The Pfizer BNT162b2 and Moderna mRNA-1273 vaccine antigens aim to address some of these important

https://doi.org/10.1021/acscentsci.1c00058
ACS Cent. Sci. 2021, 7, 586−593

factors by following a strategy first employed for MERS, as well as SARS-CoV spike vaccine design,[20,35] where two proline mutations are introduced in close proximity to the first heptad repeat of each protomer, which stabilizes the spike in its prefusion conformation.[36]

Abolishing the furin cleavage site, preventing S1 shedding, and introducing mutations to lock spike immunogens in a prefusion conformation are likely to elicit more potent antibody responses. Some vaccine candidates already combine these approaches;[6,37] one directly compared the effects of furin cleavage, stabilization, and the presence of the tPA signal sequence in vaccine efficacy. In support of our findings, the construct lacking the trimer stabilization mutations but maintaining the furin cleavage site and tPA leader sequence was the least effective of the seven platforms tested in nonhuman primates. Glycan signatures of any vaccine candidate should be compared to that of the wild-type virus. Characterizing and understanding the correct glycosylation of the virus, as we have done here, will inform vaccine design strategies and the development of a high-quality immune response, aimed at achieving the correct immunogen presentation, in this and future pandemics.

■ ASSOCIATED CONTENT

Supporting Information

Materials and Methods Figures S1−10 Movies S1 and S2 Supplementary Tables S1 and S2 The Supporting Information is available free of charge at https://pubs.acs.org/doi/10.1021/acscentsci.1c00058.

Materials and methods and additional data and figures including mascot sequence coverage, sequence alignment of S proteins, site-specific glycosylation, Western blot, MS/MS spectra, purification and glycan analysis, illustration of site-specific glycosylation changes, and flow cytometry analysis (PDF)

Movie S1: Mass photometry of $S1_{vaccine\text{-}antigen}$ (MP4)

Movie S2: Mass photometry of $S_{recombinant\text{-}trimer}$ (MP4)

■ AUTHOR INFORMATION

Corresponding Authors

Weston B. Struwe − *Physical and Theoretical Chemistry Laboratory, Department of Chemistry, University of Oxford, Oxford OX1 3TA, United Kingdom;* orcid.org/0000-0003-0594-226X; Email: weston.struwe@chem.ox.ac.uk

Nicole Zitzmann − *Oxford Glycobiology Institute, Department of Biochemistry, University of Oxford, Oxford OX1 3QU, United Kingdom;* orcid.org/0000-0003-1969-4949; Email: nicole.zitzmann@bioch.ox.ac.uk

Authors

Juliane Brun − *Oxford Glycobiology Institute, Department of Biochemistry, University of Oxford, Oxford OX1 3QU, United Kingdom;* orcid.org/0000-0002-0964-3681

Snežana Vasiljevic − *Oxford Glycobiology Institute, Department of Biochemistry, University of Oxford, Oxford OX1 3QU, United Kingdom*

Bevin Gangadharan − *Oxford Glycobiology Institute, Department of Biochemistry, University of Oxford, Oxford OX1 3QU, United Kingdom;* orcid.org/0000-0002-7466-2977

Mario Hensen − *Oxford Glycobiology Institute, Department of Biochemistry, University of Oxford, Oxford OX1 3QU, United Kingdom*

Anu V. Chandran − *Oxford Glycobiology Institute, Department of Biochemistry, University of Oxford, Oxford OX1 3QU, United Kingdom;* orcid.org/0000-0001-9942-2614

Michelle L. Hill − *Oxford Glycobiology Institute, Department of Biochemistry, University of Oxford, Oxford OX1 3QU, United Kingdom;* orcid.org/0000-0002-9289-5811

J.L. Kiappes − *Oxford Glycobiology Institute, Department of Biochemistry, University of Oxford, Oxford OX1 3QU, United Kingdom;* orcid.org/0000-0001-6697-6776

Raymond A. Dwek − *Oxford Glycobiology Institute, Department of Biochemistry, University of Oxford, Oxford OX1 3QU, United Kingdom*

Dominic S. Alonzi − *Oxford Glycobiology Institute, Department of Biochemistry, University of Oxford, Oxford OX1 3QU, United Kingdom;* orcid.org/0000-0002-1330-9109

Complete contact information is available at: https://pubs.acs.org/10.1021/acscentsci.1c00058

Author Contributions

[§]J.B. and S.V. contributed equally. B.G. and M.H. contributed equally. J.B., S.V., B.G., M.H., M.L.H., J.L.K., and D.S.A. performed experiments with data analysis support from A.V.C. and W.B.S. W.B.S. and N.Z. wrote the first draft of the manuscript with all authors contributing to revisions and editing. All authors have given approval to the final version of the manuscript.

Funding

W.B.S. acknowledges the support of the philanthropic donors to the University of Oxford's COVID-19 Research Response Fund and BBSRC/UKRI BB/V011456/1 grant (Molecular Mapping of SARS-CoV-2 and the Host Response with Multiomics Mass Spectrometry to Stratify Disease Outcomes). J.B. is supported by a Wellcome Trust PhD Programme (203853/Z/16/Z). J.L.K. is supported by a Lerner-Fink Fellowship in Medicinal Chemistry. This work was supported by the Oxford Glycobiology Endowment.

Notes

The authors declare the following competing financial interest(s): W.B.S. is a shareholder and consultant to Refeyn Ltd. All other authors declare no conflict of interest.

■ ACKNOWLEDGMENTS

We thank the Krammer Laboratory for kindly providing the spike (soluble domain) and CR3022 expression vectors, Corinne Lutomski and Tarick El-Baba (University of Oxford, Department of Chemistry) for the Krogan Laboratory full-length spike expression vector (sourced from Addgene), Anderson Ryan (University of Oxford, Department of Oncology) for Calu-3 cells, and Simon Draper (University of Oxford, Nuffield Department of Medicine) for the pENTR4-LPTOS vector. We thank Protein Metrics for software support. Figures 1 and 4 were created with the aid of BioRender.com. We thank Sarah Karin Wideman, Felix Clemens Richter, and Johannes Pettmann for technical assistance for Flow Cytometry.

■ ABBREVIATIONS

ACE-2, angiotensin-converting enzyme 2; COVID-19, coronavirus disease 2019; CMV, cytomegalovirus; ER, endoplasmic reticulum; ERGIC, ER−Golgi intermediate compartment; FACS, fluorescence activated cell sorting; GalNAc, *N*-acetylgalactosamine; HILIC, hydrophilic interaction liquid chromatography; MS, mass spectrometry; M-6-P, mannose-6-phosphate; MERS, Middle East respiratory syndrome; NTD, N-terminal domain; RBD, receptor binding domain; SARS-CoV-2, severe acute respiratory syndrome coronavirus 2; S, spike; tPA, tissue plasminogen activator; UHPLC, ultra-high-performance liquid chromatography

■ REFERENCES

(1) Shang, J.; Wan, Y.; Luo, C.; Ye, G.; Geng, Q.; Auerbach, A.; Li, F. Cell Entry Mechanisms of SARS-CoV-2. *Proc. Natl. Acad. Sci. U. S. A.* **2020**, *117* (21), 11727.

(2) Letko, M.; Marzi, A.; Munster, V. Functional Assessment of Cell Entry and Receptor Usage for SARS-CoV-2 and Other Lineage B Betacoronaviruses. *Nat. Microbiol.* **2020**, *5* (4), 562−569.

(3) Casalino, L.; Gaieb, Z.; Goldsmith, J. A.; Hjorth, C. K.; Dommer, A. C.; Harbison, A. M.; Fogarty, C. A.; Barros, E. P.; Taylor, B. C.; Mclellan, J. S. Beyond Shielding: The Roles of Glycans in the SARS-CoV-2 Spike Protein. *ACS Cent. Sci.* **2020**, *6*, 1722.

(4) Wrapp, D.; Wang, N.; Corbett, K. S.; Goldsmith, J. A.; Hsieh, C. L.; Abiona, O.; Graham, B. S.; McLellan, J. S. Cryo-EM Structure of the 2019-NCoV Spike in the Prefusion Conformation. *Science (Washington, DC, U. S.)* **2020**, *367* (6483), 1260−1263.

(5) Watanabe, Y.; Bowden, T. A.; Wilson, I. A.; Crispin, M. Exploitation of Glycosylation in Enveloped Virus Pathobiology. *Biochim. Biophys. Acta, Gen. Subj.* **2019**, *1863* (10), 1480−1497.

(6) Mercado, N. B.; Zahn, R.; Wegmann, F.; Loos, C.; Chandrashekar, A.; Yu, J.; Liu, J.; Peter, L.; McMahan, K.; Tostanoski, L. H. Single-Shot Ad26 Vaccine Protects against SARS-CoV-2 in Rhesus Macaques. *Nature* **2020**, *586* (7830), 583−588.

(7) Walls, A. C.; Tortorici, M. A.; Frenz, B.; Snijder, J.; Li, W.; Rey, F. A.; DiMaio, F.; Bosch, B. J.; Veesler, D. Glycan Shield and Epitope Masking of a Coronavirus Spike Protein Observed by Cryo-Electron Microscopy. *Nat. Struct. Mol. Biol.* **2016**, *23* (10), 899−905.

(8) Yang, T. J.; Chang, Y. C.; Ko, T. P.; Draczkowski, P.; Chien, Y. C.; Chang, Y. C.; Wu, K. P.; Khoo, K. H.; Chang, H. W.; Danny Hsu, S. Te. Cryo-EM Analysis of a Feline Coronavirus Spike Protein Reveals a Unique Structure and Camouflaging Glycans. *Proc. Natl. Acad. Sci. U. S. A.* **2020**, *117* (3), 1438−1446.

(9) Sanders, R. W.; Derking, R.; Cupo, A.; Julien, J. P.; Yasmeen, A.; de Val, N.; Kim, H. J.; Blattner, C.; de la Peña, A. T.; Korzun, J. A Next-Generation Cleaved, Soluble HIV-1 Env Trimer, BG505 SOSIP.664 Gp140, Expresses Multiple Epitopes for Broadly Neutralizing but Not Non-Neutralizing Antibodies. *PLoS Pathog.* **2013**, *9* (9), e1003618.

(10) Folegatti, P. M.; Ewer, K. J.; Aley, P. K.; Angus, B.; Becker, S.; Belij-Rammerstorfer, S.; Bellamy, D.; Bibi, S.; Bittaye, M.; Clutterbuck, E. A.; et al. Safety and Immunogenicity of the ChAdOx1 NCoV-19 Vaccine against SARS-CoV-2: A Preliminary Report of a Phase 1/2, Single-Blind, Randomised Controlled Trial. *Lancet* **2020**, *396* (10249), 467−478.

(11) van Doremalen, N.; Lambe, T.; Spencer, A.; Belij-Rammerstorfer, S.; Purushotham, J. N.; Port, J. R.; Avanzato, V. A.; Bushmaker, T.; Flaxman, A.; Ulaszewska, M.; et al. ChAdOx1 NCoV-19 Vaccine Prevents SARS-CoV-2 Pneumonia in Rhesus Macaques. *Nature* **2020**, *586* (7830), 578−582.

(12) Helenius, A.; Aebi, M. Intracellular Functions of N-Linked Glycans. *Science* **2001**, *291*, 2364−2369.

(13) Stertz, S.; Reichelt, M.; Spiegel, M.; Kuri, T.; Martínez-Sobrido, L.; García-Sastre, A.; Weber, F.; Kochs, G. The Intracellular Sites of Early Replication and Budding of SARS-Coronavirus. *Virology* **2007**, *361* (2), 304−315.

(14) Klein, S.; Cortese, M.; Winter, S. L.; Wachsmuth-Melm, M.; Neufeldt, C. J.; Cerikan, B.; Stanifer, M. L.; Boulant, S.; Bartenschlager, R.; Chlanda, P. SARS-CoV-2 Structure and Replication Characterized by in Situ Cryo-Electron Tomography. *Nat. Commun.* **2020**, *11* (1), 1−10.

(15) Hoffmann, M.; Kleine-Weber, H.; Pöhlmann, S. A Multibasic Cleavage Site in the Spike Protein of SARS-CoV-2 Is Essential for Infection of Human Lung Cells. *Mol. Cell* **2020**, *78* (4), 779−784.e5.

(16) Bosshart, H.; Humphrey, J.; Deignan, E.; Davidson, J.; Drazba, J.; Yuan, L.; Oorschot, V.; Peters, P. J.; Bonifacino, J. S. The Cytoplasmic Domain Mediates Localization of Furin to the Trans-Golgi Network En Route to the Endosomal/Lysosomal System. *J. Cell Biol.* **1994**, *126* (5), 1157−1172.

(17) Ghosh, S.; Dellibovi-Ragheb, T. A.; Kerviel, A.; Pak, E.; Qiu, Q.; Fisher, M.; Takvorian, P. M.; Bleck, C.; Hsu, V.; Fehr, A. R.; et al. *β*-Coronaviruses Use Lysosomes for Egress Instead of the Biosynthetic Secretory Pathway. *Cell* **2020**, *183*, 1520−1535.

(18) Thaysen-Andersen, M.; Packer, N. H. Site-Specific Glycoproteomics Confirms That Protein Structure Dictates Formation of N-Glycan Type, Core Fucosylation and Branching. *Glycobiology* **2012**, *22* (11), 1440−1452.

(19) Hang, I.; Lin, C. W.; Grant, O. C.; Fleurkens, S.; Villiger, T. K.; Soos, M.; Morbidelli, M.; Woods, R. J.; Gauss, R.; Aebi, M. Analysis of Site-Specific N-Glycan Remodeling in the Endoplasmic Reticulum and the Golgi. *Glycobiology* **2015**, *25* (12), 1335−1349.

(20) Pallesen, J.; Wang, N.; Corbett, K. S.; Wrapp, D.; Kirchdoerfer, R. N.; Turner, H. L.; Cottrell, C. A.; Becker, M. M.; Wang, L.; Shi, W.; et al. Immunogenicity and Structures of a Rationally Designed Prefusion MERS-CoV Spike Antigen. *Proc. Natl. Acad. Sci. U. S. A.* **2017**, *114* (35), E7348−E7357.

(21) Amanat, F.; Stadlbauer, D.; Strohmeier, S.; Nguyen, T. H. O.; Chromikova, V.; McMahon, M.; Jiang, K.; Arunkumar, G. A.; Jurczyszak, D.; Polanco, J.; et al. A Serological Assay to Detect SARS-CoV-2 Seroconversion in Humans. *Nat. Med.* **2020**, *26* (7), 1033−1036.

(22) Struwe, W. B.; Chertova, E.; Allen, J. D.; Seabright, G. E.; Watanabe, Y.; Harvey, D. J.; Medina-Ramirez, M.; Roser, J. D.; Smith, R.; Westcott, D.; et al. Site-Specific Glycosylation of Virion-Derived HIV-1 Env Is Mimicked by a Soluble Trimeric Immunogen. *Cell Rep.* **2018**, *24* (8), 1958−1966.e5.

(23) Cao, L.; Pauthner, M.; Andrabi, R.; Rantalainen, K.; Berndsen, Z.; Diedrich, J. K.; Menis, S.; Sok, D.; Bastidas, R.; Park, S. K. R. Differential Processing of HIV Envelope Glycans on the Virus and Soluble Recombinant Trimer. *Nat. Commun.* **2018**, *9* (1), 3693.

(24) Behrens, A.-J.; Harvey, D. J.; Milne, E.; Cupo, A.; Kumar, A.; Zitzmann, N.; Struwe, W. B.; Moore, J. P.; Crispin, M. Molecular Architecture of the Cleavage-Dependent Mannose Patch on a Soluble HIV-1 Envelope Glycoprotein Trimer. *J. Virol.* **2017**, *91* (2), e01894-16.

(25) Yao, H.; Song, Y.; Chen, Y.; Wu, N.; Xu, J.; Sun, C.; Zhang, J.; Weng, T.; Zhang, Z.; Wu, Z.; et al. Molecular Architecture of the SARS-CoV-2 Virus. *Cell* **2020**, *183* (3), 730−738.e13.

(26) Sanda, M.; Morrison, L.; Goldman, R. N- And O-Glycosylation of the SARS-CoV-2 Spike Protein. *Anal. Chem.* **2021**, *93*, 2003.

(27) Shajahan, A.; Supekar, N. T.; Gleinich, A. S.; Azadi, P. Deducing the N- and O-Glycosylation Profile of the Spike Protein of Novel Coronavirus SARS-CoV-2. *Glycobiology* **2020**, *30*, 981.

(28) Watanabe, Y.; Allen, J. D.; Wrapp, D.; McLellan, J. S.; Crispin, M. Site-Specific Glycan Analysis of the SARS-CoV-2 Spike. *Science* **2020**, *369* (6501), 330−333.

(29) Ramasamy, M. N.; Minassian, A. M.; Ewer, K. J.; Flaxman, A. L.; Folegatti, P. M.; Owens, D. R.; Voysey, M.; Aley, P. K.; Angus, B.; Babbage, G. Safety and Immunogenicity of ChAdOx1 NCoV-19 Vaccine Administered in a Prime-Boost Regimen in Young and Old Adults (COV002): A Single-Blind, Randomised, Controlled, Phase 2/3 Trial. *Lancet* **2020**, *396*, 1979.

(30) Rerks-Ngarm, S.; Pitisuttithum, P.; Nitayaphan, S.; Kaewkungwal, J.; Chiu, J.; Paris, R.; Premsri, N.; Namwat, C.; de Souza, M.; Adams, E.; et al. Vaccination with ALVAC and AIDSVAX

https://doi.org/10.1021/acscentsci.1c00058
ACS Cent. Sci. 2021, 7, 586−593

to Prevent HIV-1 Infection in Thailand. *N. Engl. J. Med.* **2009**, *361* (23), 2209−2220.
(31) Bukreyev, A.; Yang, L.; Fricke, J.; Cheng, L.; Ward, J. M.; Murphy, B. R.; Collins, P. L. The Secreted Form of Respiratory Syncytial Virus G Glycoprotein Helps the Virus Evade Antibody-Mediated Restriction of Replication by Acting as an Antigen Decoy and through Effects on Fc Receptor-Bearing Leukocytes. *J. Virol.* **2008**, *82* (24), 12191−12204.
(32) Mohan, G. S.; Li, W.; Ye, L.; Compans, R. W.; Yang, C. Antigenic Subversion: A Novel Mechanism of Host Immune Evasion by Ebola Virus. *PLoS Pathog.* **2012**, *8* (12), e1003065.
(33) Tortorici, M. A.; Beltramello, M.; Lempp, F. A.; Pinto, D.; Dang, H. V.; Rosen, L. E.; McCallum, M.; Bowen, J.; Minola, A.; Jaconi, S.; et al. Ultrapotent Human Antibodies Protect against SARS-CoV-2 Challenge via Multiple Mechanisms. *Science (Washington, DC, U. S.)* **2020**, *370* (6519), 950.
(34) Barnes, C. O.; Jette, C. A.; Abernathy, M. E.; Dam, K. M. A.; Esswein, S. R.; Gristick, H. B.; Malyutin, A. G.; Sharaf, N. G.; Huey-Tubman, K. E.; Lee, Y. E. SARS-CoV-2 Neutralizing Antibody Structures Inform Therapeutic Strategies. *Nature* **2020**, *588*, 682.
(35) Kirchdoerfer, R. N.; Wang, N.; Pallesen, J.; Wrapp, D.; Turner, H. L.; Cottrell, C. A.; Corbett, K. S.; Graham, B. S.; McLellan, J. S.; Ward, A. B. Stabilized Coronavirus Spikes Are Resistant to Conformational Changes Induced by Receptor Recognition or Proteolysis. *Sci. Rep.* **2018**, *8* (1), 15701.
(36) Walsh, E. E.; Frenck, R. W.; Falsey, A. R.; Kitchin, N.; Absalon, J.; Gurtman, A.; Lockhart, S.; Neuzil, K.; Mulligan, M. J.; Bailey, R. Safety and Immunogenicity of Two RNA-Based Covid-19 Vaccine Candidates. *N. Engl. J. Med.* **2020**, *383*, 2439.
(37) Keech, C.; Albert, G.; Cho, I.; Robertson, A.; Reed, P.; Neal, S.; Plested, J. S.; Zhu, M.; Cloney-Clark, S.; Zhou, H. Phase 1−2 Trial of a SARS-CoV-2 Recombinant Spike Protein Nanoparticle Vaccine. *N. Engl. J. Med.* **2020**, *383*, 2320.
(38) Soltermann, F.; Foley, E. D. B.; Pagnoni, V.; Galpin, M.; Benesch, J. L. P.; Kukura, P.; Struwe, W. B. Quantifying Protein−Protein Interactions by Molecular Counting with Mass Photometry. *Angew. Chem., Int. Ed.* **2020**, *59* (27), 10774−10779.
(39) Alonzi, D. S.; Neville, D. C. A.; Lachmann, R. H.; Dwek, R. A.; Butters, T. D. Glucosylated Free Oligosaccharides Are Biomarkers of Endoplasmic-Reticulum α-Glucosidase Inhibition. *Biochem. J.* **2008**, *409* (2), 571.

■ NOTE ADDED AFTER ASAP PUBLICATION

This paper was published ASAP on March 31, 2021. Revised on April 1, 2021 with changes to title, abstract, and last paragraph of the introduction to make it clear that the authors did not use the AstraZeneca vaccine expression material but rather used one they prepared in-house that is similar to AstraZeneca's. Revised on April 8, 2021 with changes to abstract, synopsis, last paragraph of the introduction, figure captions, and supporting information PDF to incorporate terminology consistent with independent study. Revisions have no impact on the overall data or conclusions presented.

https://doi.org/10.1021/acscentsci.1c00058
ACS Cent. Sci. 2021, 7, 586−593